International Conference on Mathematics, Computational Methods & Reactor Physics (M&C 2009)
Saratoga Springs, New York, May 3-7, 2009, on CD-ROM, American Nuclear Society, LaGrange Park, IL (2009)

A PERTURBATION RESPONSE FUNCTION GENERATION METHOD

Dingkang Zhang and Farzad Rahnema*
Georgia Institute of Technology
Corresponding Address
Dingkang.zhang@gatech.edu; Farzad@gatech.edu

ABSTRACT

This paper presents a perturbation response function generation technique for incident flux/current response expansion methods used in coarse mesh transport problems. In this approach, the forward and adjoint local problems with appropriate boundary conditions are first solved to obtain the response functions for each unique coarse mesh at a reference eigenvalue k_0, and then the response functions for an arbitrary eigenvalue k can be computed as a perturbation from the initial eigenvalue k_0. The method has been implemented into the coarse mesh neutron transport code COMET and tested for a 2-D CANDU problem. The comparisons of the response functions with those directly generated by the original method have shown that the perturbation method can significantly improve the computational efficiency in the pre-computation phase (response function calculations) while maintaining the same accuracy. The response functions generated by the perturbation method are also used for 2-D CANDU core calculations. Both the core eigenvalue and pin-power distribution are found to agree very well with the MCNP reference solutions.

Key Words: Transport theory, Coarse mesh transport method, Perturbation method, Response functions, Reactor core simulation

1. INTRODUCTION

The coarse mesh transport (COMET) method [1-2] has been recently used to provide neutronics analysis for various reactor cores [3-6] or to predict the dose delivered to human tissues [7-8]. This method is based on the incident flux expansion theory and therefore the solution to a heterogeneous global problem can be equivalently constructed by generating local solutions (or response functions) to each individual coarse mesh. The COMET method is highly accurate as long as the expansion of the angular flux or current on coarse mesh boundaries can sufficiently represent the actual phase space distribution. Extensive benchmark calculations [3-5] against the Monte Carlo code MCNP [9] for various reactor cores such as PWRs, BWRs and CANDUs have demonstrated that it can achieve high computational efficiency while maintaining an accuracy comparable to the Monte Carlo method.

The COMET method is highly efficient in terms of the core-level calculations, because the extensive computational effort at the lattice level to generate the response function library is shifted to the pre-computation phase, which could be very time-consuming, especially if high order expansions are necessary. In this paper, a perturbation method is introduced to significantly improve the computational efficiency of the response function generation method.

* Corresponding author

The paper is organized as follows. The perturbation response function method is presented in section 2. Section 3 describes the numerical implementation and benchmark calculations against MCNP reference solutions. The conclusions and future work are discussed in section 4.

2. RESEPONSE FUNCTION PERTURBATION METHOD

According to the particle balance on one of the bounding surfaces, the outgoing flux/current from a coarse mesh is the sum of the all incoming fluxes/currents that will contribute, taking into the account the possibility of the incident neutrons and their secondary scattering/fission neutrons escaping from that given surface.

$$\psi_{sm}^{+} = \sum_{s',m'} R_{m'm}^{s's}\left(k\right)\psi_{s'm'}^{-} \tag{1}$$

where $\psi_{sm}^{\pm}$ is the *m-th* moment (expansion coefficient) of outgoing/incoming flux on surface *s*, $R_{s's}^{m'm}$ represents the surface-to-surface response function, and *k* is the global eigenvalue. Since *k* is not known a *priori* before we actually solve the global problem, conventionally the response functions are calculated at a set of predefined *k* values and then interpolation is used to determine the response functions at any given eigenvalue. The linear interpolation method has been shown to be very accurate, but we must pre-compute and store a set of response functions at a number of discrete eigenvalues.

In order to improve the computational efficiency, it is possible to pre-compute the response functions only at a given global eigenvalue k_0 and then use perturbation theory to obtain the response functions at any other value. Suppose that $R_{s's}^{m'm}\left(k_0\right)$ is the response function for a coarse mesh V_i at eigenvalue k_0, then $R_{s's}^{m'm}\left(k_0\right)$ can be calculated as [1]:

$$R_{s's}^{m'm}\left(k_0\right) = \int_{\partial V_{is}} d\vec{r} \int_{\hat{\Omega}\cdot\vec{n}_{is}>0} d\hat{\Omega} \int dE \left(\hat{\Omega}\cdot\vec{n}_{is}\right) R_{s'}^{m'}\left(\vec{r},\hat{\Omega},E;k_0\right)\Gamma_m\left(\vec{r},\hat{\Omega},E\right) \tag{2}$$

where $\vec{n}_{is}$ is the unit norm on surface *s* of coarse mesh *i*, and the surface-to region response function $R_{s'}^{m'}\left(\vec{r},\hat{\Omega},E;k_0\right)$ is a local solution to the following local problem.

$$\mathbf{H}R_{is'}^{m'}\left(\vec{r},\hat{\Omega},E;k_0\right) = \frac{1}{k_0}\mathbf{F}R_{is'}^{m'}\left(\vec{r},\hat{\Omega},E;k_0\right) \tag{3}$$

with boundary conditions

$$R_{is'}^{m'}\left(\vec{r},\hat{\Omega},E;k_0\right) = \begin{cases} \Gamma_{m'}, & \vec{r}\in\partial V_{is'} \text{ and } \hat{\Omega}\cdot\vec{n}_{is'}<0 \\ 0, & \text{otherwise.} \end{cases} \tag{4}$$

where Γ_m is a set of orthogonal functions (e.g. tensor products of Legendre polynomials), where *s'* indexes the interfaces and boundary segments that comprise the boundary of coarse-mesh V_i, and δ is the Kronecker delta, and operators **H** and **F** are defined below

$$\mathbf{H} = \hat{\Omega}.\nabla + \sigma_t\left(\vec{r},E\right) - \int_0^\infty dE' \int_{4\pi} d\hat{\Omega}' \;\; \sigma_s\left(\vec{r},\hat{\Omega}',E' \to \hat{\Omega},E\right) \tag{5}$$

$$\mathbf{F} = \frac{1}{4\pi}\chi\left(\vec{r},E\right)\int_0^\infty dE' \int_{4\pi} d\hat{\Omega} v\sigma_f\left(\vec{r},E'\right) \tag{6}$$

For an arbitrary eigenvalue *k*, the resulting transport equation can be written as a perturbation to Eq. (3). Defining $\lambda \equiv \lambda_0 + \varepsilon\Delta\lambda \equiv \lambda_0 + \varepsilon\left(1/k - 1/k_0\right)$ and expanding the perturbed solution as $R_{s'}^{m'}\left(w;\lambda\right) = R0_{s'}^{m'}\left(w\right) + \varepsilon R1_{s'}^{m'}\left(w\right) + O(\varepsilon^2)$, the transport equation for the first order solution is therefore written as:

$$\mathbf{H}R1_{s'}^{m'} - \lambda_0\mathbf{F}R1_{s'}^{m'} = \Delta\lambda\mathbf{F}R0_{s'}^{m'}\left(w\right) \qquad \vec{r} \in V_i \tag{7a}$$

and

$$R1_{s'}^{m'}\left(w\right) = 0 \qquad \hat{n}\cdot\hat{\Omega} < 0 \;\; \& \; \vec{r} \in \partial V_i \tag{7b}$$

If the unperturbated adjoint response function $R0_s^{*m}\left(w\right)$ is chosen to satisfy the following equation:

$$\mathbf{H}^* R0_s^{*m} = \lambda_0 \mathbf{F}^* R0_s^{*m} \qquad \vec{r} \in V_i \quad , \tag{8a}$$

and

$$R0_s^{*m}\left(w\right) = \begin{cases} \Gamma_m\left(w\right) & \hat{n}\cdot\hat{\Omega} > 0 \;\; \& \; \vec{r} \in \partial V_{is} \\ 0 & \text{otherwise} \end{cases} , \tag{8b}$$

where $\mathbf{H}^*$ and $\mathbf{F}^*$ are standard adjoint operators defined by the following equations.

$$\mathbf{H}^* = -\hat{\Omega}.\nabla + \sigma_t\left(\vec{r},E\right) - \int_0^\infty dE' \int_{4\pi} d\hat{\Omega}' \;\; \sigma_s\left(\vec{r},\hat{\Omega},E \to \hat{\Omega}',E'\right) \tag{9a}$$

$$\mathbf{F}^* = \frac{1}{4\pi} v\sigma_f\left(\vec{r},E\right)\int_0^\infty dE' \int_{4\pi} d\hat{\Omega}\chi\left(\vec{r},E'\right) \tag{9b}$$

The first order perturbation of the surface-to-surface response function can be easily derived as:

$$\Delta R_{s's}^{m'm} = \Delta\lambda \int_{V_i} dr \int_{4\pi} d\hat{\Omega} \int dE R0_s^{*m}(w)\mathbf{F}R0_{s'}^{m'}(w) \tag{10}$$

It can be seen from the above equation that we can easily calculate the perturbated response functions once the unperturbated forward and adjoint problems (8) and (10) are solved. Equations (8) ad (10) represent fixed source problems and therefore are straightforward to solve using any stochastic methods such as MCNP.

3. NUMERICAL RESULTS

The MCNP code has been modified to generate response functions. Essentially, source particles are sampled to represent a set of boundary conditions (4) and (8b) imposed on each unique mesh. The fission sources are scaled by a factor $1/k$ whenever a neutron makes a fission collision. The response functions can be tallied as the average contribution to the quantities of interest responding to a unit incoming surface source. For example, the unperturbated surface-to-surface response function is calculated as:

$$R_{s's}^{m'm}(\lambda_0) = \frac{1}{N}\sum_{n=1}^{N} W_n\left(\hat{\Omega}_n \cdot \vec{n}_{is}\right)\Gamma_m\left(\vec{r}_n, \hat{\Omega}_n, E_n\right) \tag{11}$$

Where N is the total number of source particles, W_n, $\vec{r}_n$, $\hat{\Omega}_n$, E_n are the weight, position, direction and energy of particle n when it crosses surface s. The variance of the unperturbated surface-to-surface response function is estimated simultaneously as:

$$\begin{aligned}\delta^2[R_{s's}^{m'm}(\lambda_0)] = &\frac{1}{N}\sum_{n=1}^{N}\left[W_n\left(\hat{\Omega}_n \cdot \vec{n}_{is}\right)\Gamma_m\left(\vec{r}_n, \hat{\Omega}_n, E_n\right)\right]^2 \\ &-\left[\frac{1}{N}\sum_{n=1}^{N} W_n\left(\hat{\Omega}_n \cdot \vec{n}_{is}\right)\Gamma_m\left(\vec{r}_n, \hat{\Omega}_n, E_n\right)\right]^2\end{aligned} \tag{12}$$

The perturbation method described in section 2 was implemented and tested on both the lattice-level and core-level calculations of a 2-D CANDU benchmark problem [3]. The geometrical core configuration is shown in Figure 1. The benchmark problem consists of 95 fuel assemblies and 49 moderator blocks. Reflective boundaries conditions are assumed on the left and bottom surfaces, while vacuum boundary conditions are imposed on the top and right surfaces. The lattice configuration is illustrated in Figure 2. The bundle averaged burnup distribution is shown in color in Figure 1. The corresponding burnups value for each color is listed in Table I.

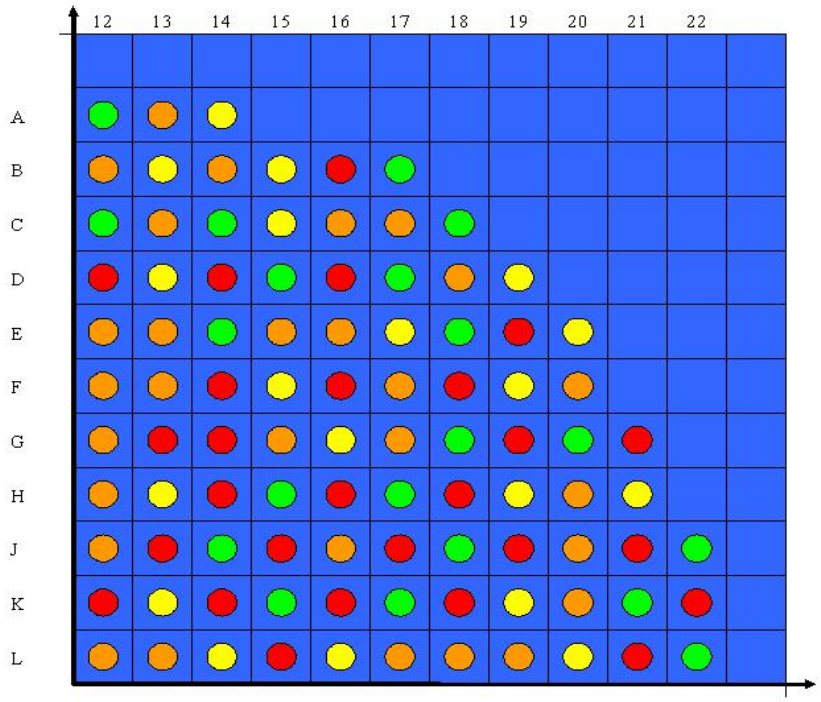

Figure 1. Quarter core representation of the 2-D Benchmark Problem

The accuracy of the perturbation response function generation method described in section 2 is assessed at both lattice and core levels in the next two sections.

Table I. Burnup Distribution Scheme for Benchmark Problems

Color Scheme	Burnup (kWd/t)	Material Properties
Green	800	Fuel I
Yellow	2700	Fuel II
Orange	5000	Fuel III
Red	7000	Fuel IV
Blue	---	Moderator

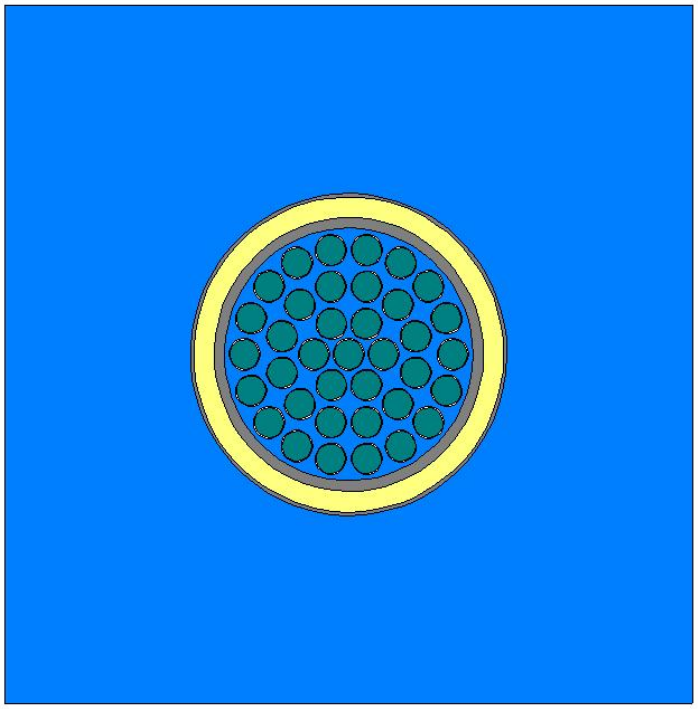

Figure 2: CANDU-6 Lattice Representation

3.1. Comparison in Lattice Level

At the core level, the modified MCNP code was first used to generate response functions at k_0=1 for five unique coarse meshes (four fuel assemblies at different burnups and one water reflector). Thirty million particle histories were used to compute the response function calculations for the forward problems. Each calculation took 6 minutes. The adjoint equation (11) at k_0=1 for each unique fuel coarse mesh was also solved by MCNP using three million particles. Each calculation took about 40 seconds. The response functions $R^{00}_{s's}\left(k=0.9\right)$ computed by the perturbation method are compared to those directly generated by MCNP in Table II. It can be seen that the maximum relative difference between the response functions for the green coarse mesh (Fuel I) calculated by the perturbation method and those directly generated by MCNP is about 0.1%, within one standard deviation of the MCNP results.

Table II. Comparison of response functions $R_{1s}^{00}(k=0.9)$ for the green coarse mesh (due to incident flux: S1G1) computed by the two methods

Outgoing flux Surface/group	Direct MCNP calculations	Perturbation Method	Relative Difference
S1/G1	5.122120E-01	5.121828E-01	0.01%
S1/G2	9.675200E-02	9.672689E-02	0.03%
S2/G1	2.687880E-02	2.685193E-02	0.10%
S2/G2	1.344948E-02	1.343853E-02	0.08%
S3/G1	1.412996E-01	1.412863E-01	0.01%
S3/G2	3.506460E-02	3.506829E-02	0.01%
S4/G1	1.412988E-01	1.412623E-01	0.03%
S4/G2	3.515080E-02	3.512487E-02	0.07%

S1: Left surface S2: Right surface
S3: Bottom surface S4: Top surface
G1: Fast group G2: Thermal group

Similar agreements were also observed for response functions (outgoing surface flux) due to the incident flux from different surfaces and groups for each unique coarse mesh. This indicates that the first order perturbation method can accurately reproduce the MCNP direct calculations for k=0.9. In order to determine under what conditions the first order approximation breaks down, the comparisons were extended to different global eigenvalues k and the results are shown in Figure 3. It can be seen that the response functions R_{11}^{00} (from the left surface to the left surface) for the green coarse mesh calculated by the perturbation method are in excellent agreement with those directly computed by MCNP when the global eigenvalue k changes from 0.5 to 1.5. While the response functions R_{12}^{00} (from the left surface to the right surface) computed by the perturbation method agree well with those directly calculated by MCNP when k changes from 0.8 to 1.3, but the relative error between the two increases to about 8% if the global eigenvalue is 0.5. The accuracy or error discrepancy can be explained by the fact that the neutrons escaping from the left surface are predominated by backscattered neutrons in the region close to the incident surface, while neutrons escaping from the right surface are dominated by fission neutrons or their progenies. As a result, when the eigenvalue k is far from the reference value of 1.0, the interactions between the perturbations in different fuel pins cannot be neglected and therefore the first order perturbation method is not sufficient for large perturbations in k.

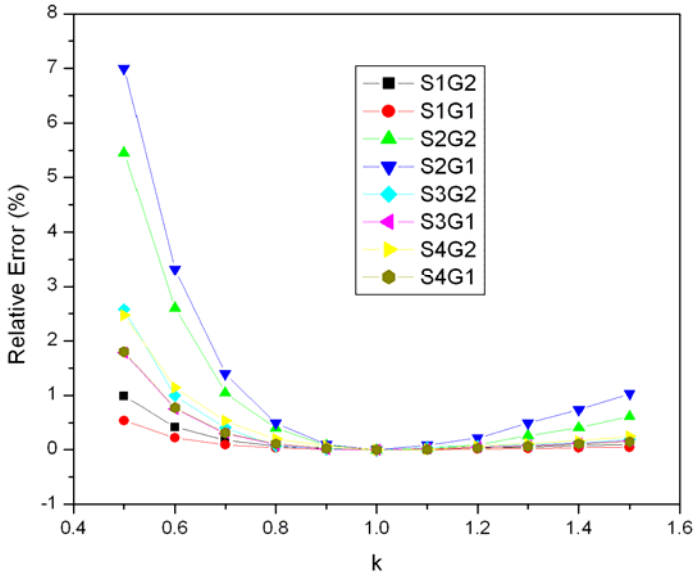

Figure 3. The relative errors of response functions generated by the perturbation method for the green coarse mesh

Since only the response functions at eigenvalue k_0 need to be directly generated by MCNP, the perturbation method is significantly faster than the original response function generation method, though extra work is incurred in solving the adjoint equation (8). Due to the fact that the first order perturbation of response functions $\Delta R_{s's}^{m'm}$ is generally at least an order of magnitude less than the unperturbated response functions $R_{s's}^{m'm}(k_0)$, the uncertainty of the response functions is then dominated by the unperturbated terms. Consequently, to maintain the same accuracy as the response functions directly generated by MCNP, much less number of particles (two orders of magnitude) are needed to solve the adjoint problems.

3.2. Comparison at the Core Level

The comparisons of response functions $R_{s's}^{00}$ in the previous section have shown the accuracy and efficiency of the perturbation method. Theoretically, an extension of the direct comparison to the higher moments of response functions is possible. However, most of the higher moments of response functions are very small and even comparable to their uncertainty, making a direct comparison impractical. For this reason, comparisons at the core level are performed to ensure the validity of the perturbation method.

Both the response function libraries generated by the perturbation method and direct Monte Carlo method were used to do whole-core calculations for the 2-D CANDU benchmark problem illustrated in Figure 1. Two-group MCNP reference calculations were also performed. The comparisons of the global eigenvalue and pin-power distributions are found in Tables III and IV, respectively.

Table III. Global Eigenvalue calculated by different methods

METHOD	GLOBAL EIGENVALUE
MCNP	1.01943 ± 0.00001
COMET {2,2,2} using the response functions generated by MCNP	1.01961± 0.00009
COMET {2,2,2} using the response functions generated by the perturbation method	1.01959± 0.00009

{a,b,c}: a^{th} order expansion in space
b^{th} order expansion in polar angle
c^{th} order expansion in azimuthal angle

Table IV: Coarse Mesh Transport {2,2,2} Results for 2-D Benchmark Problem

RESPONSE FUNCTION LIBRARY	DIRECT MCNP	PERTURBATION METHOD
Pin Power AVG (%)	0.34	0.34
Pin Power RMS (%)	0.40	0.42
Pin Power MRE (%)	0.33	0.32
Pin Power MAX (%)	0.98	1.01

RE: Relative Error
AVG: Average relative error

$$avg\ RE = \frac{\sum_{N} |e_n|}{N}$$

where N is the number of fuel pins and e_n is the calculated per cent error for the nth pin power, p_n.

RMS: Root Mean Square Error

$$RMS = \frac{\sqrt{\sum_{N} e_n^2}}{N}$$

MRE: Mean Relative Error

$$MRE = \frac{\sum_{N} |e_n| \cdot p_n}{N . p_{avg}}$$

MAX: Maximum Error

The comparisons in the core level calculations show that the perturbation method can significantly improve the computational efficiency while maintaining the same accuracy as the original method. In addition, since only the response functions at the reference eigenvalue k_0 are needed, the response function library generated by the perturbation method is significantly smaller than that directly generated by MCNP.

4. CONCLUSIONS

A perturbation method was developed to compute the first order perturbation of response functions. In this approach, the forward and adjoint response functions are first solved at an initial eigenvalue k_0, and then the response functions at an arbitrary eigenvalue k can be calculated as a perturbation from the initial state point. The method was tested on a 2-D CANDU problem at both the lattice level (response functions) and the core level (the global eigenvalue and pin-power distribution). It was shown that the perturbation method can achieve high accuracy while significantly improving the computational efficiency of the pre-computation phase. Additional benefits are the reduction in the size of the response function library (i.e., memory requirement) since in this case there is no need to generate response functions at more than one pre-defined eigenvalue.

ACKNOWLEDGMENTS

This work was supported by a grant (#DE-FC07-07ID14821) from the Department of Energy under the Nuclear Engineering Energy Research Initiative (NERI).

REFERENCES

1. S. Mosher and F. Rahnema, "The Incident Flux Response Expansion Method for Heterogeneous Coarse Mesh Transport Problems," *Transport Theory and Statistical Physics*, **34**, pp.1-26 (2006).
2. B. Forget and F. Rahnema, "COMET Solutions to the 3D C5G7 MOX Benchmark Problem," *Progress in Nuclear Energy*, **48**, pp.467-475 (2006).
3. B. Forget and F. Rahnema, "COMET Solutions to Whole Core CANDU-6 Benchmark Problem," *PHYSOR-2006: Advances in Nuclear Analysis and Simulation, American Nuclear Society's Topical Meeting on Reactor Physics*, Vancouver, BC, Canada, September 10-14 (2006).
4. B. Forget, F. Rahnema and S.W. Mosher, "A Heterogeneous Coarse Mesh Solution for the 2D NEA C5G7 MOX Benchmark Problem," *Progress in Nuclear Energy*, **45**, 2-4, pp.233-254 (2004).
5. D. Zhang and F. Rahnema, "A varied-order sweeping technique for the coarse mesh transport method," *PHYSOR-2008: International Conference on the Physics of Reactors "Nuclear Power: A Sustainable Resource"*, Casino-Kursaal Conference Center, Interlaken, Switzerland, September 14-19, 2008.
6. M. Satterfield, D. Zhang and F. Rahnema, "Evaluation of a heterogeneous coarse mesh photon transport method using a simplified lung model," *M&C conference*, Monterey, CA, April 15-19, 2007.
7. D. Zhang and F. Rahnema, F., "Coupled Photon/Electron Coarse Mesh Transport method for dose analysis in tissues," *Computational Medical Physics Working Group Workshop II*, Gainesville, Florida, Sep 30 – Oct 3, 2007.
8. J. F. Briesmeister, "MCNP – A General Monte Carlo N-Particle Transport Code, Version 4B," Los Alamos National Laboratory, *LA-12625-M* (1997).